5th European Review Meeting on Severe Accident Research (ERMSAR-2012)
Cologne (Germany), March 21-23, 2012

OECD Benchmark Exercise on the TMI-2 Plant: Analysis of an Alternative Severe Accident Scenario

G. BANDINI [1], S. WEBER [2], H. AUSTREGESILO [2], M. BUCK [3], P. DRAY [4], M. BARNACK [5], P. MATEJOVIC [5], J. H. PARK [6], H. MUSCHER [7], F. KRETZSCHMAR [7], J. DUSPIVA [8], L. SALLUS [9], J. BULLE [9], L. L. HUMPHRIES [10], M. HOFFMANN [11], H. G. LELE [12], K. DOLGANOV [13], A. KAPUSTIN [13], D. TOMASHCHIK [13], A. AMRI [14], P. GROUDEV [15], A. STEFANOVA [15]

[1] ENEA, Bologna (IT) [2] GRS, Garching (GE) [3] IKE, Stuttgart (GE)
[4] IRSN, Cadarache (FR) [5] IVS, Trnava (SK) [6] KAERI, Daejon (KO)
[7] KIT, Karlsruhe (GE) [8] NRI, Rez (CZ) [9] Tractebel, Brussels (BE)
[10] SNL, Albuquerque (US) [11] RUB, Bochum (GE) [12] BARC, Mumbai (IN)
[13] IBRAE-RAS, Moscow (RU) [14] OECD-NEA, Paris (FR) [15] INRNE, Sofia (BUL)

ABSTRACT

A benchmark exercise based on the TMI-2 plant has been launched by the Working Group on the Analysis and Management of Accidents (WGAMA) of OECD/CSNI, in conjunction with the WP 5.4 "Corium and Debris Coolability – Bringing Research Results into Reactor Applications" of the EU/SARNET-2 network of excellence, with the objective of investigating the ability of current advanced codes to predict in-vessel core melt progression and degraded core coolability. This exercise should be valuable to gather information on the capability of codes/models to predict the key phenomena during reactor severe accident of interest, by comparing the various results from several computer codes. Various severe accident sequences involving failure of safety systems or delayed operation will be investigated. These sequences will address the core reflooding issue starting from different degree of core degradation and molten material relocation into the lower plenum until vessel failure. The first severe accident sequence under investigation is a small break loss of coolant accident without recovery by emergency core cooling systems in the late phase, and thus resulting in large core melting and molten corium relocation to the lower head with possible vessel failure. In this paper the results of the first transient calculations performed by several participants in the benchmark using both mechanistic and integral codes are presented and discussed.

1 INTRODUCTION

A code to code benchmark exercise (ATMI), on a "well-defined" plant (similar to TMI-2) with prescribed boundary conditions was defined during the previous benchmark exercise proposed by the Working Group on Analysis and Management of Accidents (WGAMA). Several participants from both OECD/NEA and EU/SARNET Member countries joined that previous project. This "well-defined" benchmark scenario avoided additional and unwanted sources of discrepancies between code calculations, so as to focus on the variability of the codes calculations of core degradation [1].

Overall, the results of this exercise were quite encouraging as all the codes succeeded in calculating the scenario from the beginning to the end, with very little tuning of parameters or optimization of input decks. This showed the robustness of the computer codes and the consistency of their results as compared to twenty years ago. The code scattering observed in the calculation of some phenomena (for which physical understanding is still incomplete) revealed some model weaknesses, in particular during the reflooding phase which is crucial for the mitigation of severe accidents.

Based on the conclusions of this previous benchmark exercise, WGAMA felt it worthwhile to extend the accident analysis scope by examining the capability of the codes to predict core melt progression and the effects of SAM actions under a variety of severe accident situations in order to challenge them to the full extent of their capabilities, recognizing, however, that they are less reliable in late phase core melt progression. As current research in SARNET WP5 is focused on late phase phenomena and debris coolability, WGAMA and SARNET WP5 jointly proposed a benchmark as a follow-up to the benchmark exercise (ATMI) and which includes late phase core degradation during different severe accident sequences. This proposal was approved by the OECD/NEA Committee on the Safety of Nuclear Installations (CSNI) in December 2010.

2 FOLLOW-UP OF OECD TMI-2 BENCHMARK

2.1 Scope and objectives

Starting from the previous benchmark exercise on Alternative TMI-2 accident scenario, the present benchmark is aimed at examining different severe accident sequences involving safety system operation failure and various Severe Accident Management (SAM) measures, e.g., depressurization, delayed start of high pressure injection (HPI), loss of auxiliary feed water (AFW), etc. The impact on hydrogen production, core coolability, corium relocation into the lower plenum and vessel failure will be examined.

The proposed directions/ objectives are the following:

(i) to simulate a few selected and representative severe accident scenarios, with well defined boundary conditions, which progress to different degrees of in-vessel core melt, in order to verify the consistency of different code results on the basis of present understanding coming from severe fuel damage experiments and previous benchmarks based on experimental results, e.g., QUENCH-06, PHEBUS-FPT1, QUENCH-11, PHEBUS-FPT4;

(ii) to simulate some different branch scenarios involving SAM operations starting from the same initial conditions and accident sequence. Sequences where core reflooding occurs when the core is either almost intact or significantly melted will be examined, the objective being to check whether current SA codes are able to provide consistent and meaningful predictions to help in defining a SAM strategy, in particular by optimizing the use of available cooling water sources;

(iii) to perform some sensitivity studies on more important and uncertain key-parameters in order to evaluate their impact on core degradation, core coolability and hydrogen production; and

(iv) to extend the number of participants in order to involve more computer codes and more users. In particular, this benchmark would enhance knowledge transfer as younger code users would work under the supervision of senior ones.

The present benchmark should contribute in establishing some consensus on how the deemed confidence on the codes can be established and on what technical ground. It should also establish basis for the future work (e.g., uncertainty analysis, sensitivity analysis) in relation with important aspects of in vessel melt pool retention.

2.2 Participants and codes

The list of participants as well as the list of used computer codes is given in Table I.

Table I: participants and codes

Participant	Country	Code	Version
GRS	Germany	ATHLET-CD	Mod2.2 Cycle B
ENEA	Italy	ASTEC	V2.0R1p2-beta
IKE	Germany	ATHLET-CD	V2.2C
IRSN	France	ICARE/CATHARE	V2.3rev1
IVS	Slovakia	ASTEC	V2.0R1p2-beta
KAERI	Korea	MELCOR	-
KIT	Germany	ASTEC MELCOR	V2.0R1p2-beta -
NRI	Czech Rep.	MELCOR	-
Tractebel	Belgium	MELCOR	1.8.6
SNL	USA	MELCOR	-
RUB	Germany	ATHLET-CD	V2.2A
BARC	India	ASTEC	V2.0R1p2-beta
IBRAE RAS	Russia	SOCRAT	V3
INRNE	Bulgaria	ASTEC	V2.0R1p2-beta

3 ALTERNATIVE SEVERE ACCIDENT SCENARIO

The initial event is a small break of 20 cm^2 size in the hot leg of loop A with a simultaneous total loss of the main feed water at t = 0 s. As soon as the break opens, the primary pressure begins to decrease. After few tens of seconds, the fast steam generator (SG) dry-out with consequent loss of heat removal from the primary side results in sudden primary pressure increase. The opening of the pressurizer operated relief valve (PORV) cannot preclude the primary pressure rise and, therefore, reactor scram occurs when the pressurizer pressure set-point of 16.3 MPa is exceeded.

The auxiliary feed water starts at t = 100 s trying to restore the water in the SG up to 1 m level in a time interval of 100 s. Afterwards the SG level is maintained constant by controlling the auxiliary feed water flow rate. At the same time the SG pressure is increased up to 7.0 MPa and then maintained at this value throughout the remaining transient.

The postulated failure of the high pressure injection (HPI) and low pressure injection (LPI) systems induces the uncompensated loss of primary coolant inventory towards core uncovery, which leads to severe accident conditions. A constant make-up flow rate of 3 kg/s is performed in the cold leg during the whole transient, while there is no letdown

flow simulated, in order to reduce the uncertainty in the calculation regarding the boundary conditions with the primary system.

The primary pumps are stopped on the basis of primary coolant inventory depletion, when the primary mass falls below 85 tons. Therefore the accidental transient is let free to evolve towards core uncovery, heat-up, melting and relocation into the lower plenum, until possible lower head vessel failure.

4 CODE MODELLING FEATURES

Different models are used by the codes to represent the thermal-hydraulics (TH) behaviour in the different parts of the plant as illustrated in Table II. All codes use 1-D TH model to simulate the primary and secondary circuits' response. More detailed multi-dimensional models are generally used to simulate the core TH behaviour. Some of the codes, like ICARE/CATHARE [2], have specific multi-dimensional models developed to simulate convective movements in large volumes as for the vessel lower and upper plenum.

Table II: code thermal-hydraulic models

Code	Loop thermal-hydraulics	In-vessel thermal-hydraulics	In-core thermal-hydraulics
ASTEC	1-D	1-D	2-D
ICARE/CATHARE	1-D	3-D (azimuthally symmetric)	3-D (azimuthally symmetric)
ATHLET-CD	1-D	1-D	Multi-channels
MELCOR	1-D	1-D	Multi-channels
SOCRAT	1-D	1-D (coolant) 2-D (solid & melted structures)	Multi-channels (coolant) 2-D (solid & melted structures)

Different code models and empirical laws are used in the severe accident codes and tend to reproduce all important degradation phenomena occurring during in-vessel core melt progression, following a severe accident. These phenomena include:

1) clad deformation and burst/perforation due to creep under pressure or eutectic core material interaction at relatively low temperature,
2) clad oxidation with hydrogen generation,
3) clad failure due to zircaloy melting and oxide layer dissolution and break-up,
4) melting and relocation of metallic and ceramic core materials,
5) loss of rod-like geometry with formation of debris bed which may develop towards in-core molten pool,
6) slumping of molten core material into the lower plenum which might threaten the integrity of the vessel.

The main core degradation parameters used in the calculations by the participants are listed in Table III. The value of the different parameters has been mainly selected according to code best practice guidelines and user experience.

Table III: core degradation parameters

Participant	Zircaloy oxidation kinetics	Cladding failure criteria (e = oxide layer thickness)	Melting temperature of UO_2-ZrO_2	Debris formation criteria	Debris porosity and particle diameter
GRS	Cathcart + Urbanic	T > 2300 K and e < 0.3 mm or T > 2500 K	2600 K	2400 K	38% and 2 mm
ENEA	Cathcart + Prater	T > 2300 K and e < 0.3 mm or T > 2500 K	2550 K	2500 K	40% and 3 mm
IRSN	Cathcart + Prater	T > 2300 K and e < 0.3 mm	2550 K	2500 K	30% and 3 mm
RUB	Cathcart + Urbanic	T > 2300 K and e < 0.3 mm or T > 2500 K	2600 K	No debris bed modelling	-
IVS	Urbanic	T > 2260-2450 K and e < 0.16-0.3 mm or T > 2500 K	2830 - 2873 K	2260-2500 K	30% and 9 mm
KIT	Cathcart + Prater	T > 2300 K and e < 0.3 mm or T > 2500 K	2550 K	No debris bed modelling	-
IBRAE-RAS	Diffusion	T > 2300 K and e < 0.3 mm or T > 2500 K	UO2: 2850 K ZrO2: 2900 K U-Zr-O: 2250-2850 K	No debris bed modelling	-
BARC	Cathcart + Urbanic	T > 2300 K and e < 0.3 mm	2600 K	2600 K	60% and 3 mm
Tractebel	Urbanic	T > 2400 K and e > 0.01 mm or T > 3100 K	2800 K	2400-3100 K	40% and 2 mm
IKE	Cathcart + Urbanic	T > 2300 K and e < 0.3 mm or T > 2500 K	2600 K	No debris bed modelling	-

In general, parabolic correlations are used to calculate the oxidation of zircaloy cladding with consequent hydrogen generation. The Cathcart-Pawel correlation is mainly used in the low temperature range below 1800 K. The Prater-Courtright and Urbanic-Heidrick

correlations are used in the high temperature range above 1800 K. Specific diffusion oxidation models have been developed by IBRAE RAS in the SOCRAT code [3] in the temperature range of 1250-3000 K.

The cladding oxide scale failure with downwards relocation of metallic molten material during the early degradation phase is generally calculated on the basis of cladding temperature and the thickness of residual oxide layer (e). Most of the codes use similar parametric values for temperature and thickness.

As demonstrated by several experiments, like the Phebus FP tests, the melting point of ceramic UO_2-ZrO_2 material is lowered well below the eutectic point of the binary phase diagram (approximately 2800 K). This assumption is taken into account by most of the participants in their calculation and, thus, the melting point of fuel rods is reduced down to 2550-2600 K. Only IVS with ASTEC [4, 5], IBRAE RAS with SOCRAT and Tractebel with MELCOR [6] considered a melting temperature close to the eutectic point of ceramic materials.

More than half of the participants take into account the transition from rod-like geometry to debris bed in the core before reaching the ceramic material melting point. This is simply based on a temperature criterion. The debris bed is characterized by its porosity and particle diameter which are generally defined by code input. Different debris bed porosity and particle size values have been selected by the code users as shown in Table III. Other participants do not consider debris bed formation, because of deficiencies of current debris bed modelling in terms of the coupling to the thermal-hydraulic models in their code (ATHLET-CD calculations by RUB and IKE) or a lack of models in the code (SOCRAT calculation by IBRAE RAS), or because the debris bed model is not considered reliable enough by code developers for plant applications (ASTEC calculation by KIT).

5 CODE RESULT COMPARISON

The results of the first transient calculation submitted by most of the participants in the benchmark exercise are compared and discussed in this section. The analysed results include the steady-state condition at transient initiation, the chronology of main events during the transient phase, the thermal-hydraulics of the primary system, the in-vessel core melt progression until lower head failure and the hydrogen production. The transient calculations, and consequently the plot of the results, are stopped in case of vessel failure.

5.1 Steady-state at nominal power

The steady-state condition of TMI-2 plant at nominal power has been defined according to the final specifications of MSLB Benchmark [7], trying to achieve the best agreement in the plant state at the beginning of the calculated transient, in particular regarding the total coolant mass in the primary system. The range of calculated values of main steady-state plant parameters is compared with TMI-2 plant data in Table IV. In general, the deviations from the reference plant data are limited and considered acceptable. In particular, the maximum deviation of total primary mass is below 1.3%. The agreement on this parameter is very important, because of its impact on the timing of primary pump stop which dictates the beginning of core uncovery. The largest deviations are evidenced on pressurizer level and SG steam temperature and feed water flow rate, but they are not expected to produce significant deviations on the calculated transient evolution.

Table IV: main steady-state plant parameters

Parameter	Unit	Calculated values (range)	TMI-2 plant data
Reactor core power	MW	2772	2772
Pressurizer pressure	MPa	14.82 - 15.15	14.96
Hot leg temperature	K	589.3 - 594.8	591.15
Cold leg temperature	K	560.3 - 565.7	564.15
Primary loop flow rate	kg/s	8472 - 8888	8800
Pressurizer collapsed level	m	5.05 - 5.94	5.588
Total primary mass	kg	219830 - 225650	222808
SG secondary pressure	MPa	6.41 - 6.55	6.41
SG steam temperature	K	564.7 - 588.3	572.15
SG feed water flow rate	kg/s	701.8 - 791.0	761.1

5.2 Chronology of main events

After the initial transient phase involving reactor scram and first depressurization of the primary system down to saturation conditions, the forced circulation of liquid-steam mixture in the primary loops allows for the removal of the core decay heat as well as the pumping power through the SG secondary side. As in the real TMI-2 accident, the failure of the primary pumps is expected once the loss of primary mass compromises performance of the pumps. Based on a residual primary mass value of 85 tons, the failure of the primary pumps is calculated by all participants within a restricted range of about 230 s around t = 2205 s (see Table V).

After the failure of the primary pumps, the liquid water settles down in the primary loops and the vessel, leading to the onset of core uncovery and heat-up. The first fuel rod clad perforation/burst is predicted by ASTEC (ENEA, IVS, KIT and BARC) and MELCOR (Tractebel) codes around t = 3700 s. In general, earlier clad rupture is calculated by ASTEC due to solid eutectic interaction between zircaloy cladding and inconel grid spacers at temperature near 1100 K. The latest clad rupture is predicted by ICARE/CATHARE (IRSN) at t = 4488 s due to creep failure of pressurized fuel rod.

After clad perforation/burst the oxidation process can also be accelerated by double-side clad oxidation around the breach location. The oxidation runaway following the ZrO_2 phase change at about 1800 K results in core temperature escalation up to the melting point of zircaloy cladding, with possible oxide scale dissolution and failure and consequent mixture material dislocation. The earliest clad melting and dislocation is predicted in ASTEC calculation by IVS at 3806 s, while the latest one is predicted in the ICARE/CATHARE calculation by IRSN at t = 4921 s.

After clad melting and dislocation, the core continues to heat-up towards the ceramic material melting point. Before reaching this temperature value, transition from rod-like

geometry to porous debris bed is predicted by some of the codes used. In this case, the downward collapse of the debris bed to a less coolable configuration might accelerate the core melt progression towards the development of in-core molten pools, just above the metallic blockage area formed by refrozen materials during the early core melting and relocation phase. The earliest ceramic melting and dislocation is predicted in the ASTEC calculation by IVS at t = 4412 s, while the latest one is predicted in the ATHLET-CD calculation by RUB at t = 5203 s, likely because no transition to debris bed is modelled in the late core degradation phase.

Once hot molten materials accumulate in the core (mainly in the form of a molten pool) and spread towards the core boundaries, there is the potential for material slumping into the lower plenum via two different flow paths: at the side through the core by-pass after baffle failure or at the bottom through the core support plate. The earliest molten material slumping in the lower plenum is predicted by ASTEC (IVS) at t = 4485 s, while the latest one is predicted by SOCRAT (IBRAE RAS) at t = 7633 s.

Core material slumping in the lower plenum with the potential threat to the integrity of the lower head of the vessel is simulated in most of the calculations, except in RUB and IKE calculations with ATHLET-CD, because of the lack of specific modelling. More or less simplified models are available in the other codes, including the version of ATHLET-CD used by GRS [8]. In the calculations by GRS, ENEA, KIT and BARC the vessel failure is predicted in the time range of t = 8187 - 12123 s, while in the calculations by IRSN, IVS, IBRAE and Tractebel the vessel failure is not reached, since the thermal load on the vessel wall is likely limited by molten jet break-up during slumping and subsequent corium and debris bed cooling by water still present in the lower plenum or provided by the make-up flow rate. The earliest vessel failure is predicted in the ASTEC calculation by ENEA at t = 8187 s, while the latest one is predicted in the ASTEC calculation by KIT at t = 12123 s. The reason for the differences between these two ASTEC calculations depends on the application of debris bed modelling, which, in the ENEA calculation, accelerates the in-core material degradation and core slumping progression. Furthermore, no molten jet fragmentation model is applied in these calculations during the slumping process, which is the reason for the different lower head behaviour exhibited with respect to IVS calculation (no vessel failure).

Table V: chronology of main events

Parameter	Unit	Calculated time values (range)
Break opening and loss of SG feed water	s	0
Stop of primary pumps	s	2089 - 2320
First fuel rod clad perforation/burst	s	3642 - 4488
First clad melting and dislocation	s	3806 - 4921
First ceramic melting and dislocation	s	4412 - 5203
First molten material slumping in lower plenum (core slumping not modelled by RUB and IKE)	s	4485 - 7633
Vessel failure (not predicted in IRSN, IVS, IBRAE RAS and Tractebel calculations)	s	8187 - 12123

5.3 Plant thermal-hydraulics

The aspects relevant to plant thermal-hydraulic behaviour are illustrated from Figure 1 to Figure 5 and discussed in this section. At first, the break mass flow rate calculated by the participants is compared in Figure 1. The initial break mass flow rate decreases significantly at the beginning of the transient according with the decreasing primary pressure (see Figure 2). Once the primary pressure stabilizes at about t = 300 s according to the secondary side pressure at saturation conditions, the break flow rate (liquid and steam mixture) continues to progressively decrease due to increasing void fraction seen at the break. After primary pumps stop around t = 2200 s with consequent hot leg draining, the break flow rate switches from mixture to pure steam flow and then suddenly reduces by about 60%. From this point onwards, the break flow rate decrease is consistent with the primary pressure behaviour. All codes are able to reproduce the above described break flow rate behaviour and then the agreement among all calculations is very good (Figure 1).

After primary pumps stop and hot leg draining, the core decay heat removal by the secondary side progressively reduces down to zero, since there is no natural convection in the primary loops. Therefore, the primary pressure is no more sustained by the SG pressure and then tends to progressively reduce, as shown by all calculations in Figure 2, except for the MELCOR calculation by Tractebel, which shows a slight pressure increase at about t = 2400 s, likely because of sudden stop of decay heat removal by the secondary side.

Some significant deviations are observed in the calculated primary pressure during the core uncovery and heat-up phase from t = 3000 s onwards. Several pressure spikes are exhibited in most of the calculations and they are consistent with the timing of molten material slumping into the lower plenum and consequent strong water vaporization. As expected, the largest pressure peaks are calculated by IVS, IRSN, IBRAE RAS and Tractebel, because of molten jet break-up with enhanced thermal interaction between water and molten material. Of course, the lowest primary pressure until t = 12000 s is calculated by RUB, since no core slumping is modelled with the version of ATHLET-CD used.

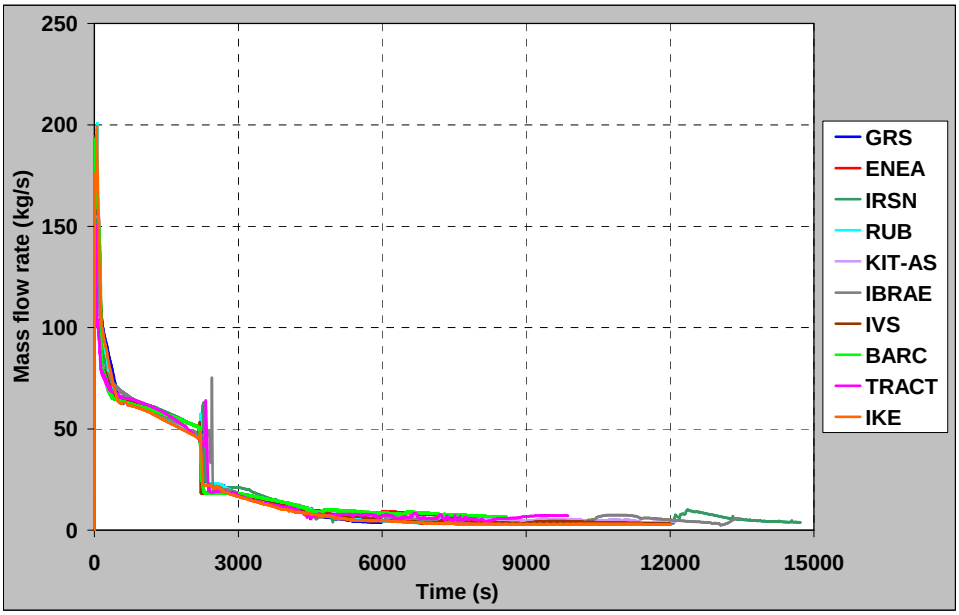

Figure 1: break mass flow rate

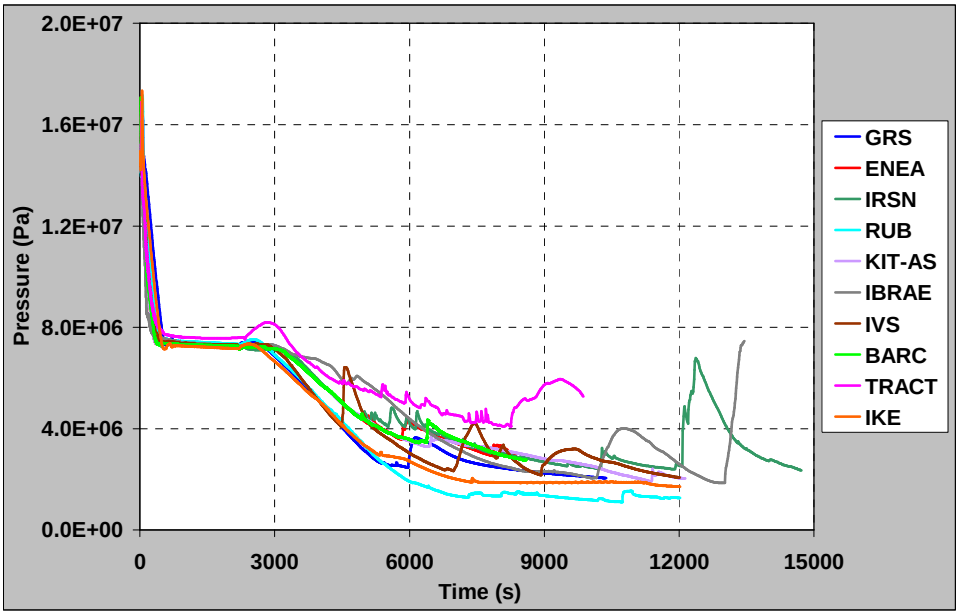

Figure 2: pressurizer pressure

The time evolution of the total primary mass of coolant is compared in Figure 3. The good agreement in the calculation of the break flow rate leads to similar agreement in calculated primary mass.

Figure 4 illustrates the time evolution of the core collapsed water level over the whole core height of 4 m for all code calculations, except for MELCOR code by Tractebel that calculates the water level over the active core height of 3.66 m. The collapsed water level reduces before primary pumps stop due to core void fraction increase. Just after the stop of primary pumps the water level suddenly increases, owing to stratification of liquid water in the lowest volumes of the primary circuit, including the vessel. This behaviour is predicted by most of the participants and codes. Afterwards the water level behaviour is in quite good agreement among all calculations.

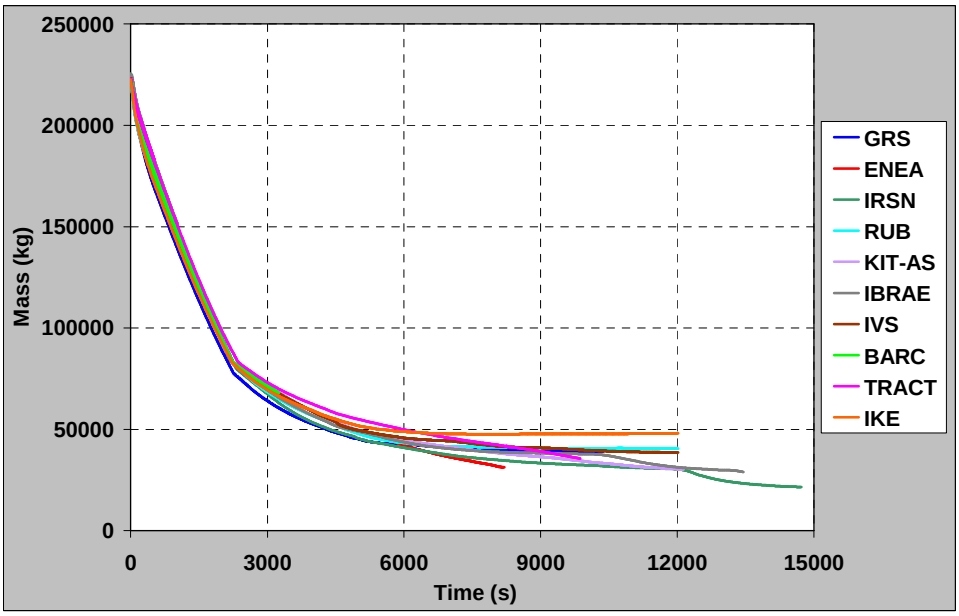

Figure 3: total primary coolant mass

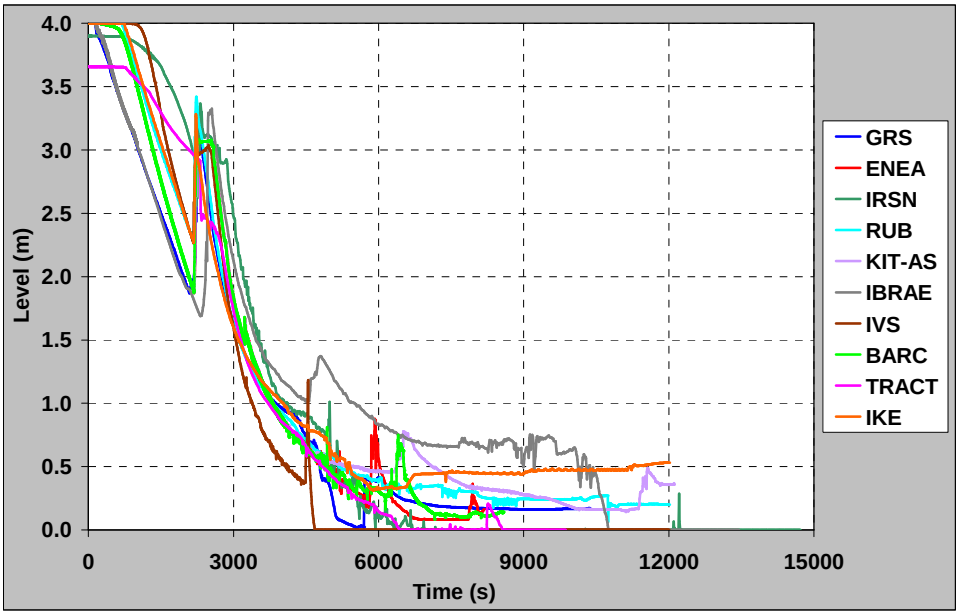

Figure 4: core collapsed level

Some water level fluctuations are, of course, calculated when molten material slumping into the lower plenum occurs. First the water level suddenly increases due to upwards displacement of water by the relocated material and then the water level reduces following strong water vaporization in the lower plenum. In some cases, due to molten jet fragmentation and strong thermal interaction with water (IRSN, IBRAE RAS, IVS and Tractebel), the water level in the vessel reduces below the bottom of the core during the core slumping phase.

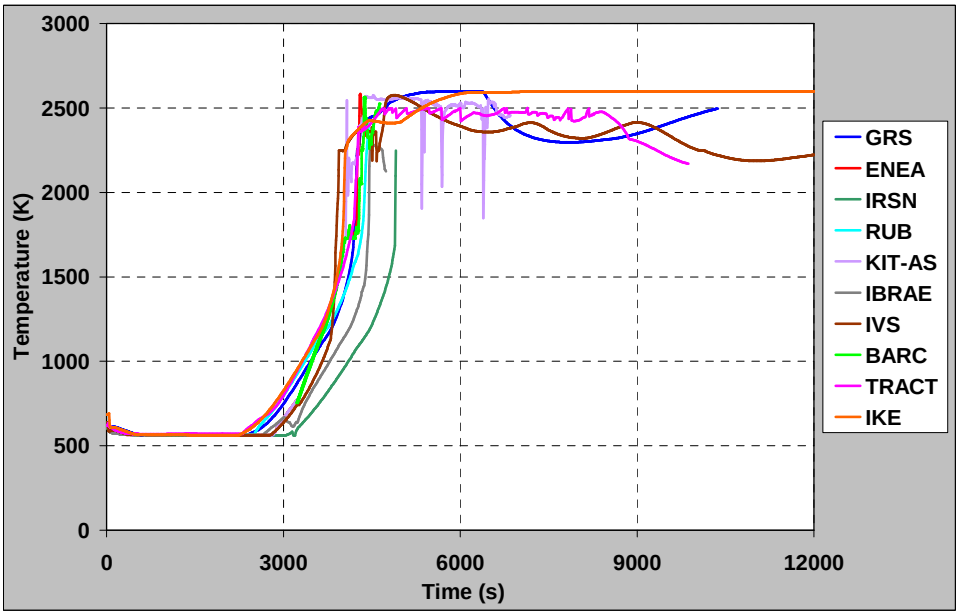

Figure 5: fuel rod clad temperature at core top

The time evolution of the fuel rod clad temperature at core top calculated in the central core channel is shown in Figure 5. The agreement in the onset of core heat-up is quite good among almost all calculations. The largest deviation is observed in the IRSN calculation with ICARE/CATHARE. This deviation is enhanced at the time of temperature escalation, likely due to 2-D convective effects within the upper plenum of the vessel,

which are taken into account only with the ICARE/CATHARE code. Furthermore, an earlier temperature escalation starting from relatively low temperature (1200 K) is calculated by IVS with ASTEC, which is likely induced by temperature escalation starting earlier at lower core levels.

In Figure 5, the plot of clad temperature is stopped once degraded fuel rod relocation occurs at the top of the core, also due to transition to debris bed and collapse. Mainly by this reason the maximum fuel rod temperature at core top is limited below 2600 K in all calculations, independently from a higher melting point of ceramic materials.

5.4 In-vessel core melt progression

The chronology of main events relevant to in-vessel core melt progression was presented and discussed previously in section 5.2. In this section the extension of core degradation and material slumping is quantified. The time evolution of total mass of degraded core material is compared in Figure 6. Several participants calculated similar amount of degraded material in the range 100-120 tons (ENEA, RUB, KIT and IRSN), even if the timing of degradation is different. IVS predicts earlier core degradation likely because of a faster core uncovery (see Figure 4). The largest degradation around 145 tons is calculated by BARC and IVS with ASTEC, likely because of enhanced debris bed formation, collapse and melting that accelerates the degradation process. The lowest degradation of about 60 tons is calculated by IKE and GRS with ATHLET-CD. In the GRS calculation, the core heating process is likely limited by the massive core slumping occurring around t = 5850 s. This effect can also explain the large deviation observed with the ATHLET-CD calculation by RUB just after core slumping. The reason why the core degradation process becomes negligible at approximately t = 7000 s in the IKE calculation should be investigated.

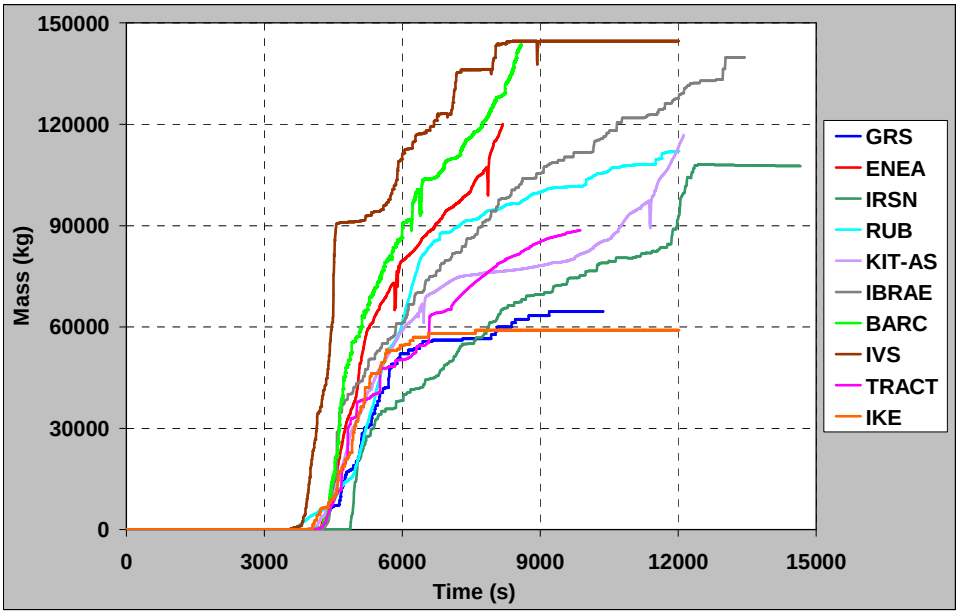

Figure 6: total mass of degraded core material

The time evolution of total mass of material relocated into the lower plenum is compared in Figure 7. The largest mass of slumped material is calculated with the SOCRAT code (117 tons). A large amount of slumped material is also calculated with ASTEC code by BARC, ENEA and KIT in the range 84-97 tons, but the timing of relocation is different; in particular it is significantly delayed in KIT calculation without in-core debris bed modelling. The smaller amount of slumped material around 45 tons is predicted by GRS with ATHLET-CD and IVS with ASTEC. IVS calculates much lower amount of slumped

material than in the other ASTEC calculations, because the baffle plate fails higher in the reactor vessel, limiting the quantity of molten material that can relocate into the lower plenum through the core by-pass.

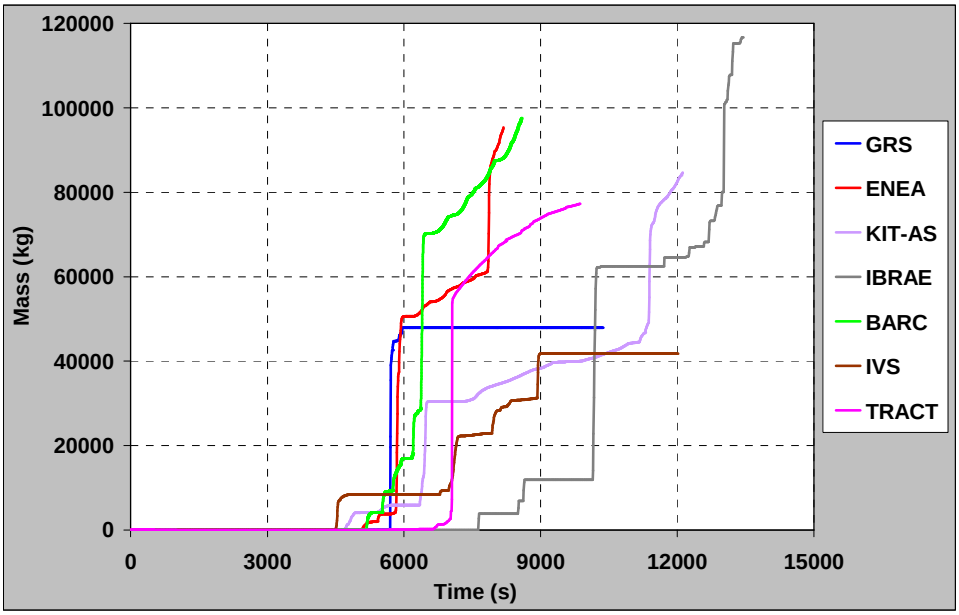

Figure 7: total mass of material relocated into the lower plenum

5.5 Hydrogen production

The time evolution of cumulative hydrogen production is compared in Figure 8. A large amount of hydrogen is predicted during the first oxidation phase in the period 4000-6000 s. Most of the participants calculate a similar amount of hydrogen at t = 6000 s in the range 300-370 kg. By this time, the lowest value of 218 kg is calculated with ICARE/CATHARE, likely due to delayed core heat-up, while the highest value of 420 kg is calculated with ASTEC by IVS.

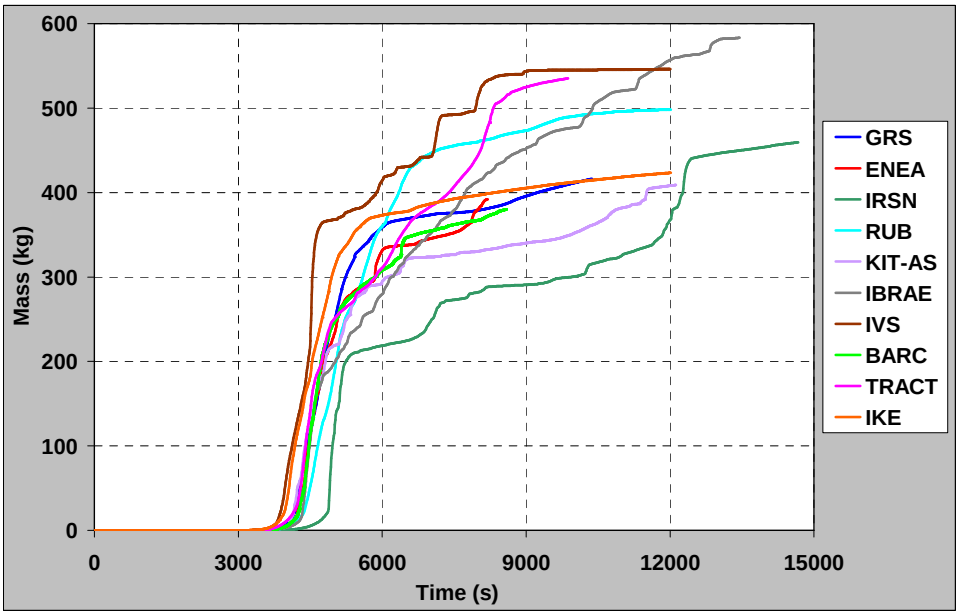

Figure 8: cumulated hydrogen production

At about 12000 s, all calculated values spread in the range 380 - 560 kg. By this time, most of the calculations were already terminated, mainly because of earlier vessel failure. Some further generation of hydrogen is predicted by IBRAE RAS with SOCRAT in the late transient phase, mainly by oxidation of metallic mixtures, up to reaching a total cumulative mass of about 580 kg after t = 13500 s.

6 CONCLUSIONS

Within the framework of the benchmark exercise on the TMI-2 plant launched by the Working Group on Analysis and Management of Accidents (WGAMA), a first severe accident sequence has been calculated by several organizations using different mechanistic and integral codes. The results of the calculations have been compared, in order to highlight the differences in code prediction of more important and key degradation phenomena, which are relevant to in-vessel core melt progression. The current calculations confirm the robustness of the codes. Indeed, all the codes were able to calculate the accident sequence up to the more severe degradation conditions.

Also, because of the harmonisation of the initial steady-state and boundary conditions, uncertainties related to the prediction of thermal-hydraulic behaviour of the plant in the first phase of the transient until the onset of core uncovery and heat-up have been minimized. This is confirmed by the rather small deviations observed in the calculations of the break flow rate and consequently, the total primary mass, which lead to an almost synchronized failure time for the primary pumps in all calculations.

Chronologically, the more significant deviations in code results are registered after the initiation of in-core melt progression and material relocation phenomena, resulting in core geometry change. The use of different core degradation parameters and late phase degradation modelling might tend to increase these differences. Sensitivity studies are ongoing in order to investigate the importance of various parameters, and try to distinguish between the influence of different core modelling features and the user effects. Furthermore, in-vessel convective movement, as in the ICARE/CATHARE calculation, could affect the core heat-up rate and the subsequent timing of core melting.

After molten core material slumping, the lower head behaviour is strongly influenced by the assumptions made in the calculations regarding molten jet break-up. Strong thermal interaction in the water-filled lower plenum might lead to more or less coolable debris bed and molten pool configuration, which may significantly delay or even exclude the vessel failure occurrence.

REFERENCES

[1] F. Fichot, O. Marchand, G. Bandini, H. Austregesilo, M. Buck, M. Barnak, P. Matejovic, L. Humphries, K. Suh, S. Paci, Ability of Current Advanced Codes to Predict Core Degradation, Melt Progression and Reflooding - Benchmark Exercise on an Alternative TMI-2 Accident Scenario, NEA/CSNI/R(2009)3 (2009)

[2] P. Drai, O. Marchand, F. Fichot, P. Chatelard, O. Coindreau, S. Belon, L. Cloarec, N. Chikni, ICARE/CATHARE V2.3rev1 - User's Manual and Guidelines, DPAM-SEMCA-2010-398 (2010)

[3] L. Bolshov, V. Strizhov, SOCRAT – The System of Codes for Realistic Analysis of Severe Accidents, Proceedings of ICAPP ’06 Reno, NV USA, June 4-8, 2006, Paper 6439 (2006)

[4] J. P. Van Dorsselaere, C. Seropian, P. Chatelard, F. Jacq, J. Fleurot, P. Giordano, N. Reinke, B. Schwinges, H.J. Allelein, W. Luther, The ASTEC integral code for severe accident simulation, Nuclear Technology, vol.165, March 2009

[5] G. Bandini, M. Buck, W. Hering, L. Godin-Jacqmin, G. Ratel, P. Matejovic, M. Barnak, G. Paitz, A. Stefanova, N. Trégourès, G. Guillard, V. Koundy, Recent advances in ASTEC validation on circuit thermal-hydraulic and core degradation, Progress in Nuclear Energy, 52, p.148–157 (2010)

[6] R. O. Gauntt et al., MELCOR Computer Code Manuals Vol. 1: Primer and Users' Guide Version 1.8.6, NUREG/CR-6119, Vol. 1, Rev. 3, SNL, September 2005

[7] K. N. Ivanov, T. M. Beam, A. J. Baratta, Pressurised Water Reactor Main Steam Line Break (MSLB) Benchmark, Volume 1: Final Specifications, NEA/NSC/DOC(99)8 (1999)

[8] K. Trambauer et al., ATHLET-CD Mod 2.2 Cycle B - User's Manual, GRS-P-4 Vol. 1, May 2011